Journal Pre-proofs

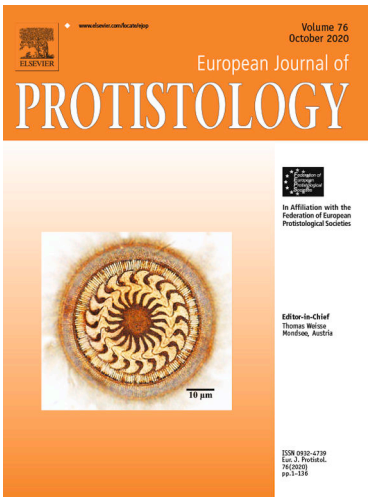


# Flow cytometric sorting of loricate choanoflagellates from the oligotrophic ocean

Nina A. Kamennaya, Gabrielle Kennaway, Barry S.C. Leadbeater, Michael A. Sleigh, Mikhail V. Zubkov

PII: S0932-4739(22)00051-7
DOI: https://doi.org/10.1016/j.ejop.2022.125914
Reference: EJOP 125914

To appear in: *European Journal of Protistology*

Received Date: 31 May 2022
Revised Date: 11 August 2022
Accepted Date: 17 August 2022

Please cite this article as: N.A. Kamennaya, G. Kennaway, B.S.C. Leadbeater, M.A. Sleigh, M.V. Zubkov, Flow cytometric sorting of loricate choanoflagellates from the oligotrophic ocean, *European Journal of Protistology* (2022), doi: https://doi.org/10.1016/j.ejop.2022.125914

# Flow cytometric sorting of loricate choanoflagellates from the oligotrophic ocean

Nina A. Kamennaya[1], Gabrielle Kennaway[2], Barry S. C. Leadbeater[3], Michael A. Sleigh[4], Mikhail V. Zubkov[5*]

[1]French Associates Institute for Agriculture and Biotechnology of Drylands, The Jacob Blaustein Institutes for Desert Research, Ben-Gurion University of the Negev, Campus Sede Boqer, 849900, Israel

[2]Imaging and Analysis Centre, Core Research Laboratories, Natural History Museum, London, SW7 5BD, United Kingdom (UK)

[3]School of Biosciences, University of Birmingham, Edgbaston, Birmingham, B15 2TT, UK

[4]Canada Road, West Wellow Nr. Romsey, Hampshire, SO51 6DD, UK

[5]Scottish Association for Marine Science, Oban, Argyll, PA37 1QA, UK

[*]Corresponding author: Mikhail Zubkov, e-mail: Mikhail.Zubkov@sams.ac.uk

**Abstract**

It is challenging to study protists with extensive, loosely-associated extracellular structures because of the problems with keeping specimens intact. Here we have tested the suitability of high-speed flow cytometric sorting as a tool for studying such protists using oceanic loricate choanoflagellates as a model. We chose choanoflagellates because their lorica-to-cell volume ratio is >10 and the voluminous loricae, i.e., the siliceous cell baskets essential for taxonomic identification, only loosely enclose the cells. Besides, owing to low concentrations, choanoflagellates are grossly under-sampled in the oligotrophic ocean. On four research cruises the small heterotrophic protists from samples collected in the photic layer of the South Atlantic and South Pacific oligotrophic (sub)tropical gyres and adjacent mesotrophic waters were flow sorted at sea for electron microscopy ashore. Among the flow-sorted protozoa we were able to select loricate choanoflagellates to assess their species diversity and concentrations. The well-preserved loricae of flow-sorted choanoflagellates made identification of 29 species from 14 genera possible. In the oligotrophic waters, we found neither endemic species nor evident morphological adaptations other than a tendency for lighter silicification of loricae. Common sightings of specimens storing extra costae in preparation for division, indicate choanoflagellates thriving in oligotrophic waters rather than enduring them. Thus, this case study demonstrates that high-speed flow sorting can assist in studying protists with extracellular structures 16-78× bigger than the enclosed cell.

**Keywords**

high-speed flow sorting, pelagic loricate choanoflagellates, morphological species diversity, extensive extracellular structures, oligotrophic ocean.

**Introduction**

Flow cytometric sorting is the physical separation of individual cells with selected optical characteristics from other cells. Initially designed for separating specific blood cells, flow sorting has been applied with minor modifications for separating prokaryotic and eukaryotic cells from various mixtures including natural waters. Although flow sorting has been used extensively, its capacity to retrieve loosely-associated extracellular structures complete with the included cells has not been explored to our knowledge. To test this capacity, we used high-speed flow sorting for studying pelagic loricate choanoflagellates in the open ocean.

Choanoflagellates (Choanoflagellatea) are heterotrophic flagellates with a characteristic collar of microvilli, which surrounds the single flagellum to form a choana (funnel) used for capturing prey. Loricate choanoflagellates produce siliceous costal strips internally and then accumulate them externally prior to building a lorica, a three-dimensional array of costae organized into a rigid basket, which loosely encloses the cell outside the organic coating (Leadbeater, 2015). Structural features of loricae allow morphological taxonomic identification of loricate choanoflagellates to a species level thus far congruent with molecular-based taxonomy (Nitsche et al., 2017). Their lorica volume exceeds cell volume at least by a factor 10. That is why we chose loricate choanoflagellates as a model for examining the effect of high-speed flow sorting on the integrity of cells with delicate extracellular structures like the lorica.

There are several hypotheses why choanoflagellates build loricae. Loricae could protect cells from predators, stabilize motion, and increase prey capture efficiency of choanoflagellates (Asadzadeh et al., 2019). Apparently choanoflagellates have particularly high capture efficiency of food-particles (Fenchel 1982; Geider and Leadbeater, 1988), including bacterioplankton and detrital particles <0.2 μm size, even at lower concentrations. Owing to such unparalleled feeding

efficiency choanoflagellates could be the chief bacterivores in the vastest biome on Earth – the oligotrophic ocean, where the bacterioplankton prey concentrations are considerably lower than in more productive oceanic regions (Zubkov et al., 2000). The oligotrophic ocean covers ~40% of the Earth's surface and comprises five (sub)tropical gyres: the Southern and Northern gyres of the Pacific and Atlantic Oceans and the Southern gyre of the Indian Ocean. However, our knowledge of the diversity and abundance of choanoflagellates in the oligotrophic ocean is based on a handful of reports (Chavez et al., 1990; Hoepffner and Haas, 1990; Vørs et al., 1995; Thomsen and Østergaard, 2019a; 2019b; Thomsen et al., 2020a; 2020b; Thomsen et al., 2021). It remains limited despite implementation of molecular techniques, mainly because of insufficient taxonomic coverage of curated reference databases for oceanic species (Leadbeater, 2015).

The limited coverage could derive from rarity of loricate choanoflagellates in the oligotrophic ocean. To study choanoflagellates seawater samples require two-stage concentrating: direct filtration followed by centrifugation of the concentrate, before the pellet is subsampled for microscopy (Vørs et al., 1995). Separation and damage of loricae during centrifugation, in addition to loss of choanoflagellates through entanglement with more abundant protists and bacteria, hampered studies of choanoflagellate diversity and particularly abundance. Here, we substituted direct filtration by reverse filtration (Zubkov et al., 1992) and centrifugation by purity flow sorting of the small heterotrophic protists, i.e., protozoa, physically separating them from bacterioplankton and phototrophic protists, i.e., algae. We examined the sorted cells using transmission and scanning electron microscopy (TEM and SEM, respectively). Flow sorting cells directly onto a filter allowed us to enumerate these cells using SEM and, hence, to determine the fraction of loricate choanoflagellates within the population of the small protozoa. Absolute concentrations of the small protozoa were determined in the original, i.e. unconcentrated, seawater samples using flow cytometry (Zubkov et al., 2007). We derived

concentrations of loricate choanoflagellates by multiplying the absolute protozoan concentrations by the fractions of loricate choanoflagellates (assuming that the fractions were unaltered by reverse filtration).

## Material and Methods

### Sampled areas

The Atlantic Ocean studies (Fig. 1) were carried out on board the Royal Research Ships (RRSs) *James Clark Ross*, *James Cook* and *Discovery IV* during the cruises JR303, JC142 and DY084 in October 2014, December 2016, and October 2017, respectively (Supplementary Table 1). Seawater samples were collected in the Atlantic mesotrophic region and South Atlantic gyre (AMR and SAG, respectively) using a rosette of 20 × 20-l Niskin bottles with the mounted CTD (conductivity, temperature, depth) profiler.

The South Pacific Ocean study (Fig. 1) was carried out on board the Research Vessel (RV) *Sonne* during the cruise SO245 ("UltraPac" expedition) in January 2016 (Supplementary Table 1). Seawater samples were collected at eight stations along a longitudinal transect through the South Pacific mesotrophic region and gyre (SPMR and SPG, respectively).

### Flow cytometry

In both the Atlantic and Pacific studies samples for flow sorting were collected from one depth (Supplementary Table 1), which either represented the surface mixed layer or the deep chlorophyll maximum (Kamennaya et al., 2022).

For flow sorting the small protozoa in the Atlantic, a large volume of seawater was collected using one of the rosette 20-l bottles. In the South Pacific we collected a large volume of seawater for flow sorting conjointly with samples for assessing microbial metabolic activities

using an acid-washed 20-l GO-FLO sampling bottle. The seawater was transferred from the bottles into acid-washed 20-l polyethylene containers and concentrated as described below.

To determine absolute concentrations of small protozoa, seawater subsamples were fixed with 1% (w/v, final concentration) cold paraformaldehyde (PFA, 20% w/v dissolved in seawater and filtered through a 0.1 μm pore size filter), stained with SYBR Green I DNA dye (Marie et al., 1997) and analysed by flow cytometry (FACScan, Becton Dickinson, Oxford, U.K.) using the CellQuest software (Zubkov et al., 2007).

Using the remaining volumes of the transferred samples cells >1 μm in diameter were gravity-concentrated by reverse-flow filtration (Zubkov et al., 1992). Briefly, water was very gently withdrawn upwards from the sample through a 1μm pore size polycarbonate filter placed above the sample, suction being provided by a small difference in hydrostatic pressure (<20 cm of water). The concentrated samples were fixed with ice-cold paraformaldehyde to 4% (w/v) final concentration, stained with 0.1 mg $l^{-1}$ Hoechst 33342 (final concentration), and kept on ice prior to flow sorting the small protozoa using the custom-configured (Kamennaya et al., 2018) MoFlo XDP instrument (Beckman-Coulter, High Wycombe, UK) and the Summit 5.4 software. Sorting purity and recovery by the instrument were controlled using blue (350/440 nm) 1.0-μm beads (Life Technologies) following manufacturer's instructions as well as by flow sorting defined populations of other microbes and subsequently confirming their morphological uniformity using electron microscopy (Kamennaya et al., 2022).

**Microscopy**

For TEM analyses of whole mount cells, 0.5-5.0×$10^3$ cells of the small protozoa were flow sorted directly onto Formvar/carbon–covered 200 mesh copper grids (Agar Scientific, Stansted, UK), stained with 2% w/v gadolinium (aqueous solution), rinsed with pure deionized water, and

stored in a desiccator for analysis ashore. The grids were examined at 200 keV with a JEOL 2011 LaB6 TEM instrument (JEOL (UK) Ltd., Welwyn Garden City, UK) fitted with a Gatan UltraScan 1000 camera (Gatan UK, Oxford, UK) at the University of Warwick or at 100 keV with a *Hitachi H-7650* TEM instrument fitted with AMT 2K × 2K digital camera system at the Bioimaging Laboratory of the Royal Botanic Gardens, Kew in London, England.

For SEM analyses, 0.6-3.0×$10^3$ cells of the small protozoa were flow sorted either into recipient 5 ml tubes (on the Atlantic cruises) or directly onto 13-mm (pore size 0.2 µm) polycarbonate filters (on the South Pacific cruise). In the first case, the tube contents were filtered onto 13-mm polycarbonate filters (pore size 0.2 µm) under low vacuum after sorting. The sorted protists deposited on filters were dehydrated in an ethanol series, and dried using 99.9% hexamethyldisilazane (Sigma-Aldrich). To minimise loss of sorted cells dehydration was performed using low-vacuum filtration (<0.1 atm) controlled by a manual pump. The dehydrated filters were stored in a desiccator at room temperature.

Prior to SEM analyses, the filters were sputtered with Au/Pd (3:2) to a thickness of 10 nm using a Cressington High-Resolution Sputter Coater coupled with an MTM20 film thickness controller (Cressington Scientific Instruments, Watford, UK). SEM imaging was carried out using a ZEISS Ultra Plus field emission SEM (Carl Zeiss microscopy UK, Cambridge, UK) at the Imaging and Analysis Centre of the Natural History Museum in London, England. Cells flow sorted from the Atlantic Ocean were located using manual search and imaged at high resolution at 5 keV. To locate clusters of cells sorted directly onto filters from the Pacific Ocean samples a low-resolution scan of whole filters was first performed using an automated motorized stage, coupled with a ZEISS ATLAS image capture system with the SEM operating at 5 keV using the

secondary electron detector. Single cells and groups of several cells were imaged at high resolution at 5 keV using the low-resolution images as navigational aids.

**Determination of cell and lorica dimensions**

Linear cell and lorica dimensions were determined from both SEM and TEM micrographs and cross-compared, where possible, using standard statistical tests. Under the assumption that a cell shape could be approximated by a triaxial ellipsoid, cell volumes were calculated as $V=\pi/6\times(l\times w\times h)$; where l = length of the longest cell dimension, w = length at 90° to the longest cell dimension or width and h = cell height or thickness was assumed equal to w (Supplementary Table 2). The lorica volume was calculated as a cone or a composite figure comprising the cone with the conjoined right circular conical frusta (Supplementary Tables 3, 4; Supplementary Fig. 1).

**Results and Discussion**

Although the small protozoa were still countable by flow cytometry in oceanic samples, their low concentrations of $10\text{-}1500\times10^3$ cells $l^{-1}$ (Fig. 2a) made direct flow sorting impractical because of 1000× higher concentrations of bacterioplankton. Therefore, we pre-concentrated protists versus bacterioplankton by reverse-flow size fractionation. Then we used high-speed flow sorting to separate smaller protozoa from bacterioplankton and algae (Fig. 3). The separated protozoa were subsequently analysed using SEM and TEM. To estimate concentrations of loricate choanoflagellates (Fig. 2) we counted the sorted cells using SEM micrographs at lower and intermediate magnifications (Fig. 4a, b).

High-resolution electron microscopy revealed that the integrity of loricae was relatively well preserved allowing for a morphological species identification of flow sorted

choanoflagellates (Figs. 4-7; Table 1; Supplementary Table 1; Supplementary Figs. 1, 2). Linear cell and lorica dimensions, i.e., height ahd width (Fig. 8a; Supplementary Tables 2, 3), were determined manually using SEM micrographs of higher resolution (Fig. 4c) to calculate their volumes (Fig. 8b; Supplementary Table 4). The dimensions of the cell and lorica of the six choanoflagellate species that were relatively common among the flow sorted protozoa are comparable to their dimensions determined using the direct filtration-centrifugation method (Thomsen and Østergaard, 2019a; 2019b; Thomsen et al., 2020a; 2020b; Thomsen et al., 2021). The estimated ratios of their lorica-to-cell volumes were 16-78 depending on the species (Fig. 8b).

High-resolution SEM provided otherwise unobtainable information about the spatial-geometric organization of structural elements, such as junctions between siliceous costae and costal strips in the loricae of choanoflagellates (Figs. 5-7; see also Figs. 13b, c and 14e in Thomsen et al., 2021), which is essential for species identification. High-resolution TEM visualized the interaction between siliceous costae and organic cell compartments (Figs. 5a, h) as well as organization of the thinnest costae in tiny species, e.g., *Crucispina cruciformis* (Fig. 6h). The extent to which minute morphological features of the choanoflagellate lorica are conserved between specimens of the same species from the two oceans (Figs. 5-7) is noteworthy.

**Concentrations and diversity of loricate choanoflagellates**

Loricate choanoflagellates were omnipresent among protozoa flow sorted from both the Atlantic and South Pacific Oceans (Fig. 1; Table 1). Higher encounter rates on SEM filters of identifiable choanoflagellate specimens in the Pacific versus Atlantic samples is likely due to sorting cells directly onto filters during the Pacific cruise. Apart from the opportunity to study more specimens, the other advantage of sorting cells onto filters is the ability to assess ambient

concentrations of loricate choanoflagellates (Fig. 2). The total concentration of loricate choanoflagellates ranged between 10-127×$10^3$ cells $l^{-1}$ and was highest at the western fringes of the SPG (SPG_1, _2), where choanoflagellates comprised 13-15% of the community of small protozoa (Fig. 2a). At these stations choanoflagellates were ~3× more abundant than in either SPMR waters to the west or in the SPG centre to the east.

Overall, 23 and 17 species attributable to 12 and 10 genera were encountered in the Atlantic and South Pacific oceans respectively (Table 1). Nine of the genera were found at more than one location. Eighteen out of the 28 species (11 out of 14 genera) were found in at least one of the two sampled gyres. Seven species (5 out of 14 genera) were found in both SAG and SPG. For comparison, 20 species from 10 genera were encountered in the mesotrophic waters of either the Atlantic or South Pacific, of which 5 species of 4 genera were common to both.

Species from four genera, i.e., *Stephanacantha, Pleurasiga*, *Cosmoeca* and *Campyloacantha*, were found in both mesotrophic and oligotrophic waters of the Atlantic Ocean (Figs. 6, 7). Species from six genera, i.e., the four listed above plus *Coronoeca* and *Bicosta*, were found in waters of both nutritious states in the South Pacific Ocean (Figs. 2b, 5; Table 1).

At the species level, we found *Pleurasiga echinocostata*, *Cosmoeca ventricosa, Cosmoeca ceratophora* and *Campyloacantha spinifera* in both the SAG and SPG. Because these species were also reported from a range of other regions at different latitudes (Leadbeater, 2015; Thomsen and Østergaard, 2019a; 2019b; Thomsen et al., 2020a), they appear to be biogeographically cosmopolitan.

We repeatedly observed *Coronoeca conicella* in the SPG (Fig. 5b, c). Previously, it was also sighted in oligotrophic waters of the North Pacific (Hoepffner and Haas, 1990), west of Australia, in Sargasso and the Caribbean and Eastern Mediterranean Seas. *C. conicella* has also been recorded in mesotrophic waters of the Equatorial Pacific, in the Gulf of California and in

the Andaman Sea (Thomsen et al., 2021). The map of findings suggests that *Coronoeca conicella* could be a species generally common to oligotrophic waters. However, because we did not encounter *Coronoeca conicella* in samples from the Atlantic Ocean (Table 1), we could not confirm ubiquity of this recently described species (Thomsen et al., 2021) in the open ocean.

Based on structural characteristics of its lorica, *Stephanacantha zigzag* (Fig. 5l) was recently transferred from *Parvicorbicula* to the *Stephanacantha* genus (Thomsen et al., 2020b). Species of this genus are common in a pelagic realm but rarely found in coastal or inshore regions (Leadbeater, 2015) contrary to species of the *Parvicorbicula* genus. We observed *Stephanacantha zigzag* exclusively in the SAG and SPG (Table 1). Other species of the *Stephanacantha* genus dominated choanoflagellates in western fringes of the SPG (Fig. 2b). Larger cells of *Stephanacantha dichotoma*, whose protoplast was enclosed by three thin posterior costae that grouped to form a long pedicel (Figs. 5a, 6e), were less common than a morphotype of smaller cells, whose 10-11 broad petal-like costae with no pronounced pedicel formed an armour above the mid-lorica zigzag belt of thin costae (Fig. 5e; Supplementary Figs. 1a, 2a). Because sightings of this morphotype were limited to the open ocean, i.e., South and North Pacific (sub)tropical gyre, Sargasso Sea and Indian Ocean northwest of Broome in Australia, this recently described species with a lightly silicified lorica was named *Stephanacantha oceanica* (Thomsen et al., 2020b).

We were fortunate to examine >30 specimens of *Stephanacantha oceanica*, by far more than specimens of other species (Supplementary Table 1). *Stephanacantha oceanica* was encountered at the gyre fringing SPG_1, _2 stations, where this species reached concentrations of 66-78×$10^3$ cells $l^{-1}$ and comprised >50% of all loricate choanoflagelates (Fig. 2b). Species diversity of choanoflagellates at the SPG_1, _2 stations was average compared to other stations (5-6 species of 4-5 genera). The lowest diversity comprising only a single species,

*Parvicorbicula socialis*, at a concentration of merely $10\times10^3$ cells $l^{-1}$ was found at the station SPMR_2 where in contrast the highest concentration of the small protozoa, $1500\times10^3$ cells $l^{-1}$ (Fig. 2a) was observed. The highest diversity (10 species) at a total abundance of $30\times10^3$ cells $l^{-1}$ was found at the SPG_3 station closer to the gyre centre (Fig. 2b). The choanoflagellate abundance of 15-$30\times10^3$ cells $l^{-1}$ in the SPG was generally comparable to the concentrations determined in the temperate waters off-shore from Central California and in the equatorial Pacific Ocean (Chavez et al., 1990; Vørs et al., 1995). However, at the western fringes of the SPG (Fig. 2, SPG_1, _2) the choanoflagellate community was dominated by *Stephanacantha oceanica* reaching blooming concentrations comparable to concentrations of other choanoflagellate species in coastal regions (McKenzie et al., 1997).

Generally larger *Campyloacantha spinifera, Diaphanoeca pedicellata, Calliacantha multispina* and *Calliacantha simplex* with heavier silica strips were encountered in mesotrophic waters (Fig. 7, Table 1). The observed diversity suggests that choanoflagellate species common to oligotrophic oceans tend to have rather smaller loricae constructed of more lightly silicified costae (Figs. 5, 6) than choanoflagellates living in more productive oceanic regions. However, the trend for more lightly-constructed loricae was not without exceptions: *Thomsenella infundibuliformis* with petaloid silicified costae (Fig. 5d4) and large *Diaphanoeca pedicellata* (Fig. 5d2), common to cold waters (Leadbeater, 2015), both containing >50 costal strips in their loricae, were encountered in the gyres.

Flow-sorted specimens of *Parvicorbicula socialis* (Figs. 5k, 7b) retained their loricae with a circular anterior transverse costa, characteristic for specimens collected using direct filtration (Thomsen et al., 2020a). We recorded this species solely outside the gyres (Supplementary Table 1). The observed distribution pattern is in accordance with the established general absence of *P. socialis* in oligotrophic (sub)tropical waters (Leadbeater, 2015; Thomsen

and Østergaard, 2019a) and suggests that this species requires mesotrophic waters with higher prey concentrations.

**Choanoflagellate growth indication**

Actively growing cells of tectiform loricate choanoflagellates accumulate costal strips on their collars in preparation for cell division when one daughter cell, the juvenile, will use the strips to build a new lorica and the other daughter cell will inherit the parent lorica. In our samples, costal strip accumulations on collar microvilli or/and inside the cell were observed in flow-sorted specimens of many species (Figs. 5-7; Supplementary Figs. 1b, 2). Cells with costal strip accumulations were more frequent at the western fringes of the SPG (SPG_1, _2). At the station SPG_2, approximately one out of three recorded choanoflagellate cells had an accumulation of costal strips on its collar (Supplementary Fig. 2a). A higher abundance of cells preparing for division indicated a higher growth rate of loricate choanoflagellates in that area and explained their blooming concentrations (Figs. 2b, 5). Though less common, costal strip accumulations were also encountered in specimens collected from the SPG centre (Fig. 5d; SPG_3, _4). Some cells flow sorted from the SAG also had costal accumulations (Fig. 6b, f). This implies that at least some species of loricate choanoflagellates thrive in the oligotrophic gyres, for instance, specimens of *Cosmoeca* genus in particular commonly had costal accumulations (Figs. 5d1, h, 6f, 7i; Supplementary Fig. 2b). Hence, common sightings of specimens preparing for division reflect efficient predation and growth of choanoflagellates in the oligotrophic ocean.

**Conclusions**

The well-preserved loricae remain attached to their accompanying cells during flow sorting and this permitted analysis of choanoflagellate diversity and abundance in the oligotrophic ocean,

advancing our knowledge about choanoflagellate biogeography and ecology. Also, flow sorting provided enough intact specimens for morphometry of commoner species. Hence, using the oceanic loricate choanoflagellates as a model, we demonstrate the ability of flow sorting to reproducibly separate protists together with loosely-associated extracellular structures 16-78 times bigger than their attached cells.

**Acknowledgement**

The authors acknowledge the chief and fellow scientists, the captains, officers and crew aboard the RRSs James Clark Ross, James Cook and Discovery IV for their help during the JR303, JC142 and DY084, respectively. The authors further acknowledge the chief and fellow scientists (from the Max Planck Institute for Marine Microbiology, Bremen), the captain, officers and crew aboard the RV SONNE for help during the SO245. The authors are especially grateful to the RV SONNE chief engineer Achim Schüler for his invaluable help with fast sorter pneumatics. The authors are very grateful to Peter Burkill for inspiring high-speed flow sorting at sea and to Vitalii Zubkov for his help with making the containerised flow sorting laboratory seaworthy. The authors thank Priscila Lange and Ivo Tews for their help with the flow cytometry analyses on the JR303 and SO245, respectively. The authors thank Ian Hands-Portman from the University of Warwick, Tomasz Goral and Alex Ball from the Natural History Museum, London and Chrissie Prychid from the Royal Botanical Gardens, Kew in London for their help with the electron microscopy imaging. This study was supported by the UK Natural Environment Research Council (NERC) Research Grants (NE/M014363/1 and NE/M011186/1) and the Max Planck Society.

**References**

Asadzadeh S.S., Nielsen, L.T., Andersen, A., Dölger, J., Kiørboe, T., Larsen, P.S., Walther, J.H., 2019. Hydrodynamic functionality of the lorica in choanoflagellates. J. R. Soc. Interface 16, 20180478.

Chavez, F.P., Buck, K.R., Barber, R.T., 1990. Phytoplankton taxa in relation to primary production in the equatorial Pacific. Deep Sea Res. A 37, 1733-1752.

Fenchel, T., 1982. Ecology of heterotrophic microflagellates. I. Some important forms and their functional morphology. Mar. Ecol. Prog. Ser. Oldendorf 8, 211-223.

Geider, R.J., Leadbeater, BSC., 1988. Kinetics and energetics of growth of the marine choanoflagellate *Stephanoeca diplocostata*. Mar. Ecol. Prog. Ser. Oldendorf 47, 169-177.

Hoepffner, N., Haas, L.W., 1990. Electron microscopy of nanoplankton from the North Pacific Central Gyre. J. Phycol. 26, 421-439.

Kamennaya, N.A., Kennaway, G., Fuchs, B.M., Zubkov, M.V., 2018. Pomacytosis—Semi-extracellular phagocytosis of cyanobacteria by the smallest marine algae. PLoS Biol. 16, e2003502.

Kamennaya, N.A., Kennaway, G., Sleigh, M.A., Zubkov, M.V., 2022. Notable predominant morphology of the smallest most abundant protozoa of the open ocean revealed by electron microscopy. J. Plankton Res., in press.

Leadbeater, B.S.C., 2015. The Choanoflagellates: Evolution, Biology, and Ecology. Cambridge, UK, Cambridge University Press.

Marie, D., Partensky, F., Jacquet, S., Vaulot, D., 1997. Enumeration and cell cycle analysis of natural populations of marine picoplankton by flow cytometry using the nucleic acid stain SYBR Green I. Appl. Environ. Microbiol. 63, 186-193.

McKenzie, C.H., Deibel, D., Thompson, R.J., MacDonald, B.A., Penney, R.W., 1997. Distribution and abundance of choanoflagellates Acanthoecidae in the coastal cold ocean of Newfoundland, Canada. Mar. Biol. 129, 407-416.

Nitsche, F., Thomsen, H.A., Richter, D.J., 2017. Bridging the gap between morphological species and molecular barcodes – Exemplified by loricate choanoflagellates. Eur. J. Protistol. 57, 26-37.

Thomsen, H.A., Østergaard, J.B., 2019a. Loricate choanoflagellates Acanthoecida from warm water seas. II. *Bicosta*, *Apheloecion*, *Campyloacantha*, *Crucispina*, *Calliacantha* and *Saroeca*. Eur. J. Protistol. 67, 114-131.

Thomsen, H.A., Østergaard, J.B., 2019b. Loricate choanoflagellates Acanthoecida from warm water seas. IV. *Cosmoeca* Thomsen. Eur. J. Protistol. 71, 125632.

Thomsen, H.A., Kamennaya, N.A., Zubkov, M.V., Østergaard, J.B., 2020a. Loricate choanoflagellates Acanthoecida from warm water seas. VI. *Pleurasiga* Schiller and *Parvicorbicula* Deflandre. Eur. J. Protistol. 75, 125717.

Thomsen, H.A., Kamennaya, N.A., Zubkov, M.V., Østergaard, J.B., 2020b. Loricate choanoflagellates Acanthoecida from warm water seas. VII. *Calotheca* Thomsen and Moestrup, *Stephanacantha* Thomsen and Syndetophyllum Thomsen and Moestrup. Eur. J. Protistol. 76, 125728.

Thomsen, H.A., Hara, S., Østergaard, J.B., 2021. Loricate choanoflagellates Acanthoecida from warm water seas. IX. *Coronoeca* gen. nov., *Polyfibula* Manton and spiny forms of *Parvicorbicula* Deflandre. Eur. J. Protistol. 81, 125826.

Vørs, N., Buck, K.R., Chavez, F.P., Eikrem, W., Hansen, L.E., Østergaard, J.B., Thomsen, H.A., 1995. Nanoplankton of the equatorial Pacific with emphasis on the heterotrophic protists. Deep Sea Res. 2 42, 585-602.

Zubkov, M.V., Burkill, P.H., Topping, J.N., 2007. Flow cytometric enumeration of DNA-stained oceanic planktonic protists. J. Plankton Res. 29, 79-86.

Zubkov, M.V., Sazhin, A.F., Flint, M.V., 1992. The microplankton organisms at the oxic-anoxic interface in the pelagial of the Black Sea. FEMS Microbiol Ecol. 10, 245-250.

Zubkov, M.V., Sleigh, M.A., Burkill, P.H., Leakey, R.J.G., 2000. Picoplankton community structure on the Atlantic Meridional Transect: a comparison between seasons. Prog. Oceanogr. 45, 369-386.

**Figure legends**

**Figure 1**. Schematic map of the South Pacific and Atlantic Oceans showing the location of sampling stations marked by dotted grey and white triangles with apices upwards and downwards to indicate the mesotrophic and oligotrophic waters, respectively.

**Figure 2.** (a) Concentrations of the small heterotrophic protists (sHP) including loricate choanoflagellates (Cho-L) in samples collected at stations in the South Pacific mesotrophic waters (SPMR) and gyre (SPG). (b) Concentrations of the 15 species that comprised the loricate choanoflagellates at these stations. Loricate choanoflagellates collected at the station SPG_5, were identified using non-quantitative TEM method and, hence, are not shown at (a).

**Figure 3.** Example of flow cytometric plot of the concentrated, DNA-stained oceanic microbes for targeted flow sorting of the small heterotrophic protists (sHP). (a) A dot plot of $10^5$ dots of Hoechst-DNA fluorescence (FL1) excited by the first 355 nm laser versus shallow angle or forward light scatter (FSC) showing the dominating bacterioplankton population above the set threshold and scatter of the small protists. The grey oval indicates 1.0-µm reference beads. (b) A dot plot of $10^5$ dots of Hoechst-DNA fluorescence (FL1) versus red fluorescence (FL4) excited by the first laser showing the bacterioplankton and small protists. The grey oval indicates 1.0-µm reference beads. The dark grey lines indicate the zoomed into area shown on the plot (c). (c) A dot plot of $2\times10^6$ dots of Hoechst-DNA fluorescence (FL1) versus red fluorescence (FL4) excited by the first laser showing the bacterioplankton and small protists with the dominant population of sHP, indicated by the blue polygon. Notice the scale change to amplify the targeted sHP population and 1.0-µm reference beads (grey oval).

**Figure 4**. SEM micrographs exemplifying (a) a cluster of flow sorted cells of the small heterotrophic protists imaged at low-magnification. (b) Intermediate magnification micrograph of four choanoflagellates marked with white arrowheads. (c) Measurements of lorica and cell dimensions of a choanoflagellate cell (*Pleurasiga minima*): arrows – length and width of a protoplast, dash-dot lines – height and width of a lorica, punctuated line – flagellum length, curly brackets – length of collar microvilli.

**Figure 5**. TEM (a, h) and SEM (b-g, i-m) micrographs of the identified species of loricate choanoflagellates flow sorted from the South Pacific Ocean: (a) *Stephanacantha dichotoma* Thomsen 1983; (b, c) *Coronoeca conicella* Thomsen, Hara & Østergaard 2021; (d1) *Cosmoeca ceratophora* Thomsen 1984, (d2) *Thomsenella acuta (Thomsen, 1983) Thomsen and Østergaard, 2019*, (d3) *Pleurasiga minima* Throndsen 1970, (d4) *Thomsenella infundibuliformis* (Leadbeater, 1974) Özdikmen, 2009; (e) *Stephanacantha oceanica* Thomsen 2021; (f, m) *Campyloacantha spinifera* (Leadbeater 1973) Hara & Takahashi 1987; (g) *Spinoeca buckii* Thomsen, Østergaard & Hansen 1995; (h) *Cosmoeca ceratophora* Thomsen 1984; (i) *Cosmoeca ventricosa* Thomsen 1984; (j) *Pleurasiga minutissima* Thomsen 2020; (k) *Parvicorbicula socialis* (Meunier 1910) Deflandre 1960; (l) *Stephanacantha zigzag* (Thomsen, 1991) Thomsen et al., 2020; (m) *Campyloacantha spinifera* (Leadbeater 1973) Hara & Takahashi 1987. Accumulations of costal strips on collar microvilli (labelled with white arrows) are recorded for *Cosmoeca ventricosa* (d1) and *C. ceratophora* (j), *Thomsenella infundibuliformis* (d4), *Stephanacantha oceanica* (e), and *Pleurasiga minima* (j). Scale bar = 2 µm unless otherwise marked.

**Figure 6**. SEM (a-g, i, j) and TEM (h) micrographs of the identified species of loricate choanoflagellates flow sorted from the (sub)tropical Atlantic Ocean: (a) *Pleurasiga minima*

Throndsen 1970; (b) *Pleurasiga echinocostata* Espeland 1986; (c) *Stephanacantha parvula* Thomsen 1983; (d) *Campyloacantha spinifera* (Leadbeater 1973) Hara & Takahashi 1987; (e) *Stephanacantha dichotoma* Thomsen 1983; (f) *Cosmoeca ceratophora* Thomsen 1984; (g) *Cosmoeca norvegica* Thomsen 1984; (h) Crucispina cruciformis (Leadbeater, 1974) Espeland and Throndsen, 1986 (i) *Crinolina aperta* (Leadbeater 1975) Thomsen 1976; (j) *Pleurasiga minutissima* Thomsen 2020. Accumulations of costal strips on collar tentacles (labelled with white arrows) are recorded for *Pleurasiga echinocostata* (b) and *Cosmoeca ceratophora* (f). Scale bar = 2 μm unless otherwise marked.

**Figure 7**. SEM micrographs of the identified species of loricate choanoflagellates flow sorted from the equatorial (f) or temperate South Atlantic Ocean: (a) *Pleurasiga echinocostata* Espeland 1986; (b) *Parvicorbicula socialis* (Meunier 1910) Deflandre 1960; (c, top) *Cosmoeca norvegica* Thomsen 1984, (c, bottom) *Calliacantha multispina* Manton & Oates 1979; (d) *Campyloacantha imbricata* Hara & Takahashi 1987; (e) *Diaphanoeca pedicellata* Leadbeater 1972; (f) *Thomsenella cercophora* (Thomsen, 1983) Thomsen and Østergaard, 2019; (g) *Pleurasiga minutissima* Thomsen 2020; (h) *Parvicorbicula circularis* Thomsen 1976; (i) *Cosmoeca sp.* ventricosa form D with extended costal tips and accumulation of costal strips on collar tentacles (labelled with white arrow); (j) *Calliacantha simplex* Manton & Oates 1979; (k) *Pleurasiga tricaudata* Booth 1990. Scale bar = 2 μm.

**Figure 8.** Comparison of cell and lorica specimen (a) and mean (b) volumes of the six choanoflagellate species most common in the open ocean (*Stephanacantha oceanica* (*S.o.*),

*Stephanacantha dichotoma* (*S.d.*), *Campyloacantha spinifera* (*C.s.*), *Coronoeca conicella* (*C.c.*), *Pleurasiga minima* (*P.mi.*) and *Pleurasiga minutissima* (*P.mu.*).

**Tables**

**Table 1.** Genera and species of loricate choanoflagellates found in the Atlantic mesotrophic region (AMR) and South Atlantic gyre (SAG), South Pacific mesotrophic region and gyre (SPMR and SPG, respectively).

| Genus | Species | AMR | SAG | SPMR | SPG |
|---|---|---|---|---|---|
| *Stephanacantha* | *oceanica* | | | | ×× |
| | *dichotoma* | | × | × | ××× |
| | *zigzag* | | × | | ×× |
| | *parvula* | × | | | |
| *Pleurasiga* | *minima* | × | | ×× | ××× |
| | *echinocostata* | × | × | × | × |
| | *minutissima* | ×× | | | × |
| | *tricaudata* | × | | | |
| *Cosmoeca* | *ventricosa* | ×× | × | × | ×× |
| | *ceratophora* | | × | × | ×× |
| | *norvegica* | × | × | | |
| | *phuketensis* | | × | | |
| *Campyloacantha* | *spinifera* | × | × | × | ××× |
| | *imbricata* | × | | | |
| *Coronoeca* | *conicella* | | | × | ××× |
| *Bicosta* | *antennigera* | | | × | |
| | *spinifera* | × | | | × |
| *Parvicorbicula* | *socialis* | × | | ×× | |
| | *circularis* | × | | | |
| *Crucispina* | *cruciformis* | | × | | × |
| *Diaphanoeca* | *pedicellata* | × | | | |
| *Calliacantha* | *multispina* | × | | | |
| | *simplex* | × | | | |
| *Thomsenella* | *acuta* | | | | × |
| | *cercophora* | × | | | |
| | *infundibuliformis* | | | | × |
| *Crinolina* | *aperta* | | × | | |
| *Apheloecion* | *quadrispinum* | | × | | |
| *Spinoeca* | *buckii* | | | | × |

× – found at one sampling location or station, ×× – found at two stations, ××× – found at three or more stations.

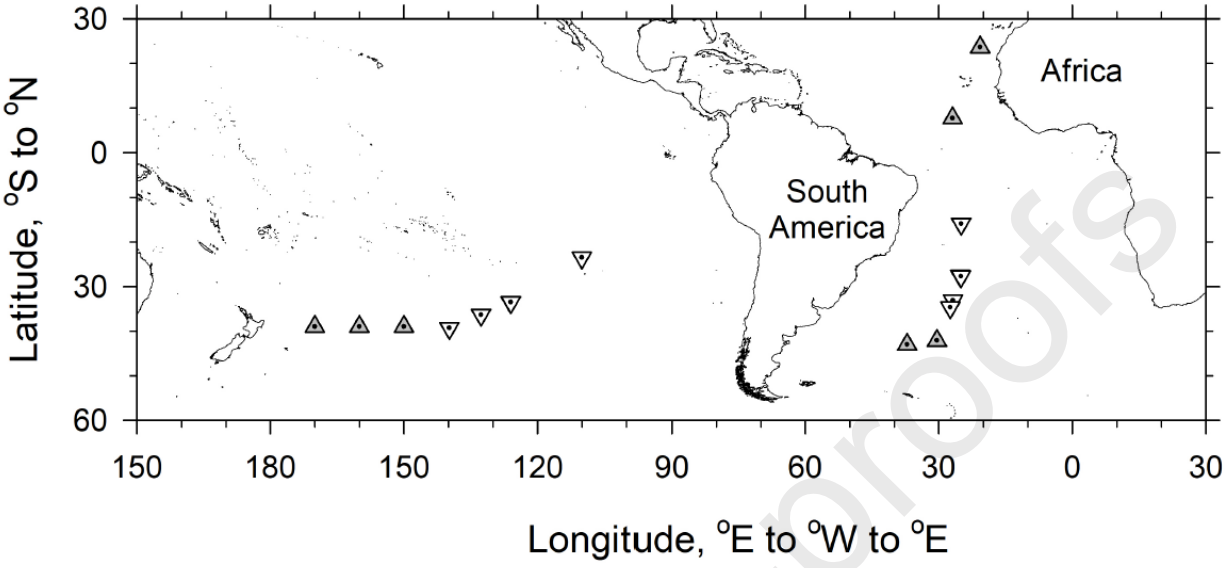

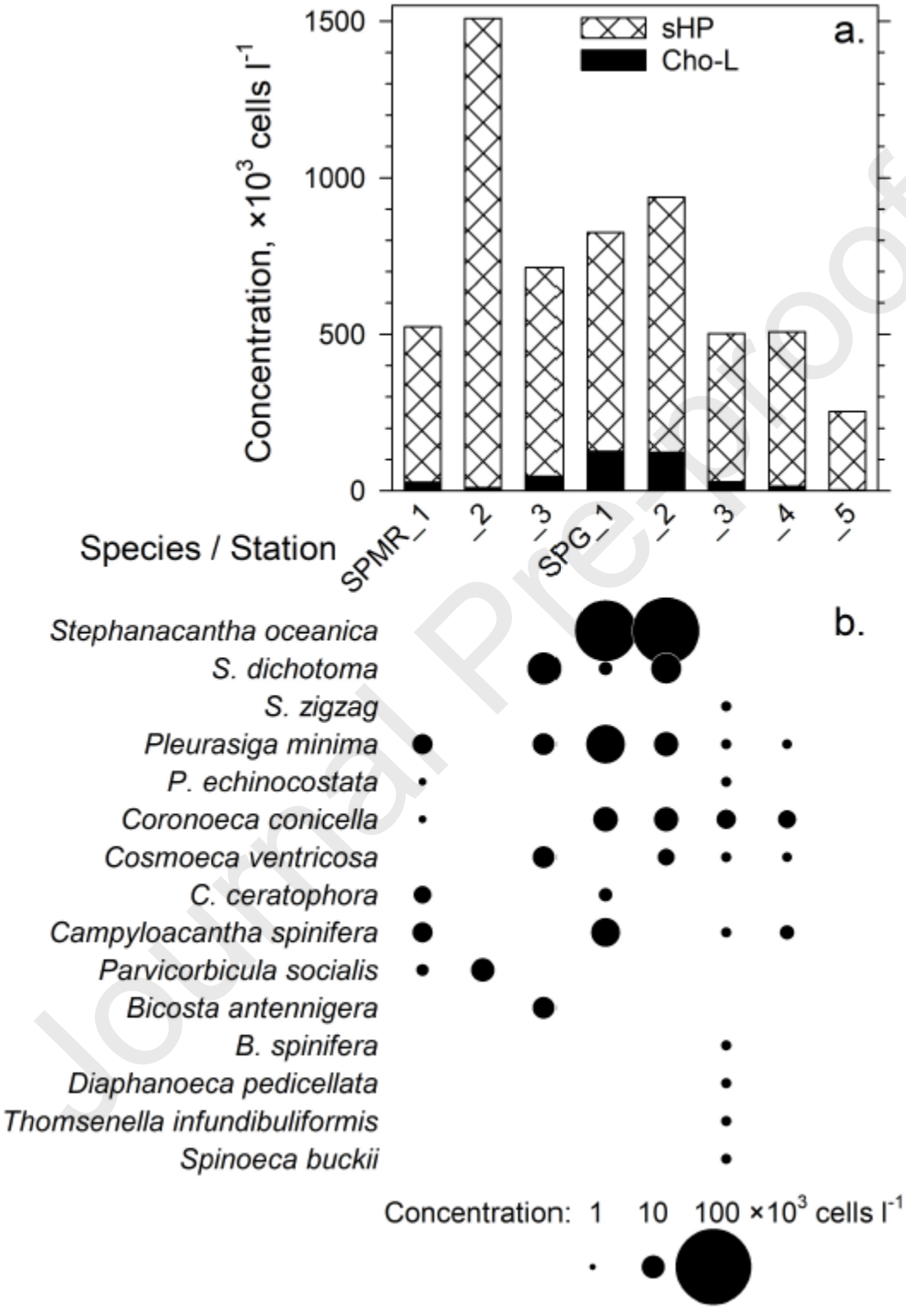

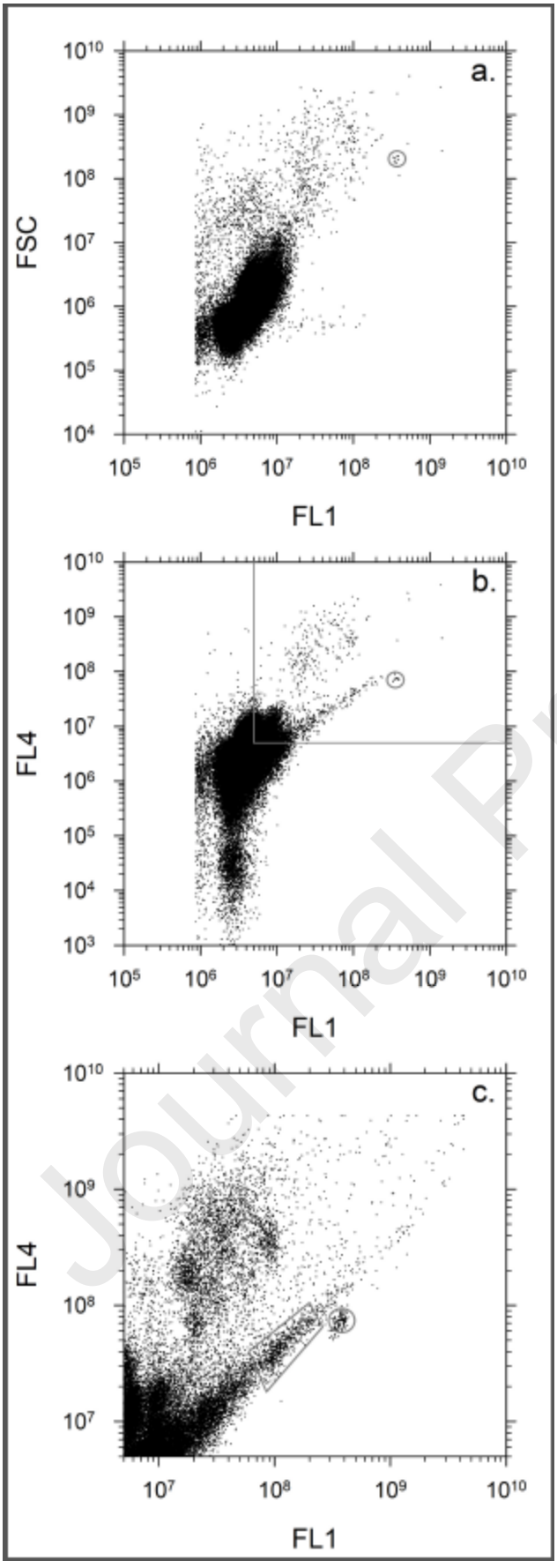

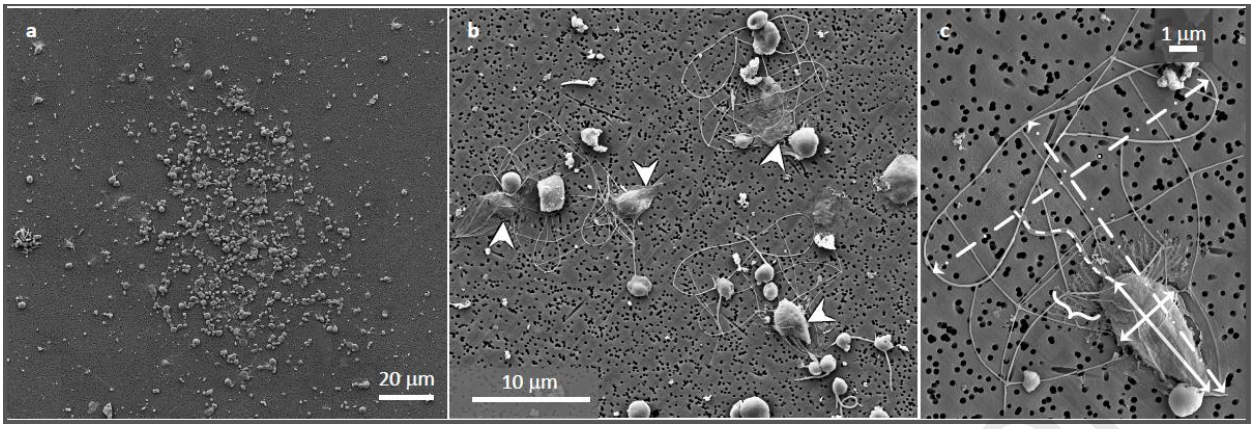

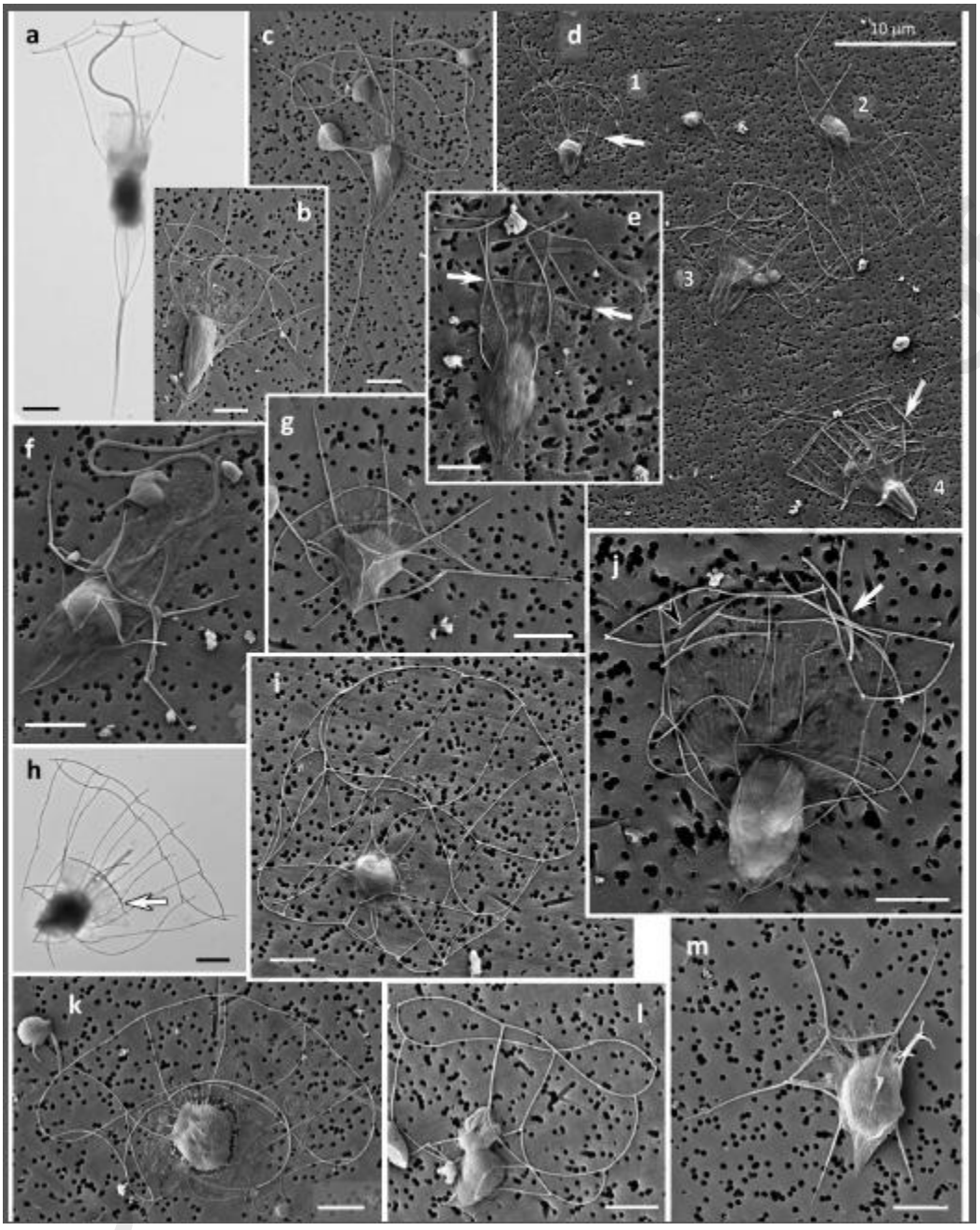
a
b
c
d
10 µm
1
2
3
4
e
f
g
h
i
j
k
l
m

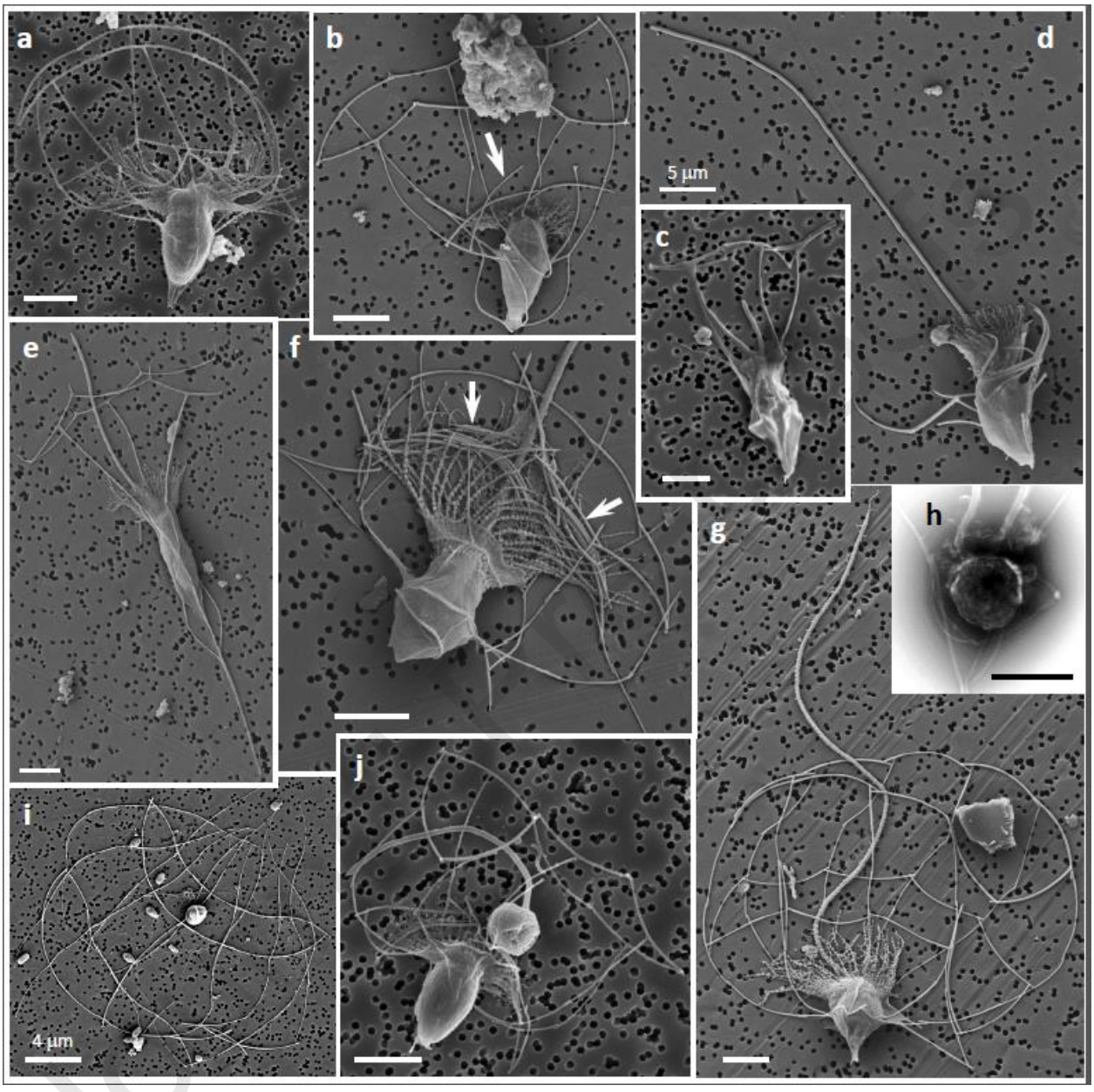
a
b
d
5 µm
c
e
f
h
g
j
i
4 µm